

Effects of Solvents on Poly(3,4-Ethylenedioxythiophene) (PEDOT) Thin Films Deposited on a (3-Aminopropyl)Trimethoxysilane (APS) Monolayer by Vapor Phase Polymerization

Mohammad Amdad Ali, Hyunho Kim, Kyunghoon Jeong, Hoesup Soh, and Jaegab Lee*

School of Advanced Materials Engineering, Kookmin University, Seoul 136-702, Korea

This study examined the effects of THF (tetrahydrofuran)-EtOH (ethanol) binary solvents on the formation of conducting poly (3,4-ethylenedioxythiophene) (PEDOT) nanofilms on (3-aminopropyl)trimethoxysilane (APS)-coated SiO₂ surfaces by vapor phase polymerization (VPP). Rutherford backscattering spectrometry (RBS) showed that the spin-coated FeCl₃ oxidants consisted of Fe, Cl, C, and O. The carbon in the oxidant film was attributed to the inclusion of solvent in the film, and the FeCl₃ oxidant spin-coated film with a THF-EtOH ratio of 1 had a higher level of C than the film spin-coated with a pure EtOH solvent. The inclusion of solvent affected the formation of the subsequent PEDOT film, thereby influencing the film properties, such as the conductivity and surface morphology. Increasing the THF/EtOH ratio to 0.5 tended to minimize the surface roughness while further increase beyond this resulted in increased surface roughness, thus indicating the existence of an optimum THF/EtOH ratio. The highest conductivity (525 S/cm) was obtained in the PEDOT films deposited with THF:EtOH (wt. %) = 1. In addition, the PEDOT films showed poor adhesion on the oxidant films deposited from a 50-50 wt. % solvent, possibly due to shielding effects of the THF solvent present between the PEDOT and APS monolayer.

PACS : 82.35.-x,73.61.Ph, 31.70.Dk

Keywords: vapor phase polymerization, conducting polymer, solvent

1. INTRODUCTION

Conducting polymers, particularly poly (3,4-ethylenedioxythiophene) (PEDOT), hold promise as electrodes for electronic devices, such as organic thin film transistors, photodiodes, organic light emitting diodes, and photovoltaic cells,^[1-5] on account of their excellent environmental stability, high optical transparency in the visible range, and moderate to high conductivity comparable with indium tin oxide (ITO).^[6-10] A range of methods have been used to polymerize PEDOT thin films, such as oxidative chemical polymerization, electrochemical polymerization, vapor phase polymerization (VPP), and spin-casting process.^[11-14] Solvents have a significant effect on the polymerization process. There have been a number of studies on the effects of solvents on polymerization and related properties of PEDOT films.

In the case of oxidative chemical polymerization, alcoholic solvents associated with the counter ions of PEDOT through hydrogen bonding cause a change in molecular ordering during polymerization.^[11,15] A shorter chain alcoholic solvent induces more effective packing of PEDOT and enhances the conductivity of the film.^[11] In addition, mor-

phological changes to the film surface are due to the presence of solvent.^[11,16] The polymerization kinetics is also influenced by the solvent. An alcoholic solvent with low viscosity favors a higher growth rate,^[17] whereas a higher evaporation rate kinetically traps the polymerization mechanism at an earlier stage.

Among the many methods, VPP has been reported to provide homogeneous and pure PEDOT films, and yield high conductivity films.^[13,18] However, the rough surface of the PEDOT films deposited using FeCl₃ oxidants in EtOH results in low conductivity films, a shortcoming that needs to be addressed. The solvent is thought to affect the reaction mechanism for PEDOT formation by controlling the activity of the oxidant. Therefore, this study examined the effects of an EtOH-THF binary solvent system on the formation of PEDOT thin films along with the resulting properties, such as surface morphology and conductivity.

2. EXPERIMENTAL

An oxidized (100) Si wafer (1.5 cm × 1.5 cm) was exposed to UV illumination (wavelength = 184 nm and 254 nm) in air for 20 min to render the surface hydrophilic. A (3-Aminopropyl) trimethoxysilane (APS) monolayer was formed on the surface by dipping the sample into 50 ml of an ethanol

*Corresponding author: lgab@kookmin.ac.kr

(EtOH) solution containing 0.1 mM (3-Aminopropyl) trimethoxysilane (APS, 97% purity), and 1 μ M acetic acid for 1 h. Subsequently, the sample was rinsed with EtOH followed by drying under blowing N_2 . A 3 wt. % $FeCl_3$ solution in a binary solvent (EtOH-THF) was spread over the monolayer surface and spun at 3000 rpm with a spin coater for 60 s. The $FeCl_3$ -coated sample was placed with the spin-coated surfaces facing downward in an EDOT deposition chamber maintained at 80°C in a mechanical circulation oven (Yuyu Scientific Mfg. Co., Korea) for 3 min to polymerize EDOT. The PEDOT sample was rinsed with methanol and dried in a desiccator prior to characterization. A four point probe (Chang Min Co., LTD, Korea) was used to measure the sheet resistance of the PEDOT film. Field emission scanning electron microscopy (FESEM) was used to examine the surface morphology and thickness of the PEDOT thin film. Atomic force microscopy (AFM, Seiko, Japan; trapping mode, scan speed: 0.5-0.6 Hz, scan size: $3 \times 3 \mu m^2$ or $10 \times 10 \mu m^2$) was used to examine the surface roughness and morphology. Rutherford backscattering spectroscopy (RBS) was used to measure the depth profiles of the elements, such as C, O, Fe, and Cl, as well as the stoichiometry of the spin-coated $FeCl_3$ films. A Fourier transform infrared (FTIR) microspectrometer was used to characterize the PEDOT nanofilms.

3. RESULTS AND DISCUSSION

PEDOT thin films were deposited on APS-coated SiO_2 surfaces with 3 wt. % $FeCl_3$ in THF-EtOH binary solvent mixtures at a chamber temperature of 80°C for 3 min. Figure 1 shows the change in conductivity of the PEDOT films as a function of wt. % of THF in the binary solvent system. For comparison, pure EtOH was used to produce a PEDOT film with a conductivity of approximately 370 S/cm. The conduc-

tivity of the film increased with increasing THF wt. % and reached a maximum of 585 S/cm at THF:EtOH (wt. %) = 1. Further increases in the THF wt. % caused a gradual decrease in conductivity.

Figure 2 shows the SEM surface morphology of the PEDOT films deposited on the APS monolayer at different THF wt.%. Different features were observed on the PEDOT films deposited at different THF:EtOH ratios. The PEDOT films deposited on the oxidant with pure EtOH had a rough surface with many tiny pores and smooth islands. The surface morphology improved significantly as the THF:EtOH ratio was increased to 1, and then degraded with further increases in the ratio. The stripe lines likely form along with smooth areas at THF:EtOH = 0.75, and then increase to cover the entire area when a pure THF solvent was used. The different surface features might be related to solvent effects on the molecular ordering of the PEDOT films, which affect

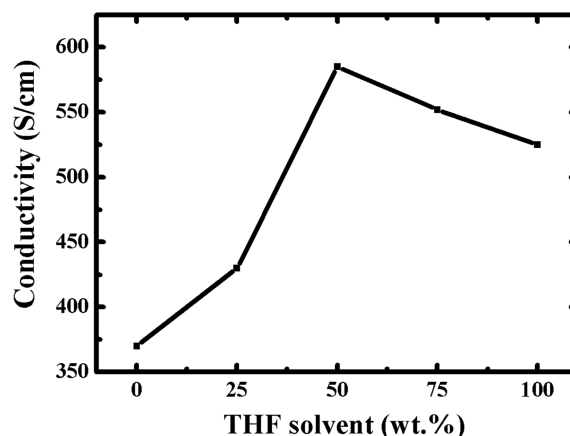


Fig. 1. Conductivity of PEDOT thin films as a function of the THF wt. % in a THF-EtOH binary solvent system.

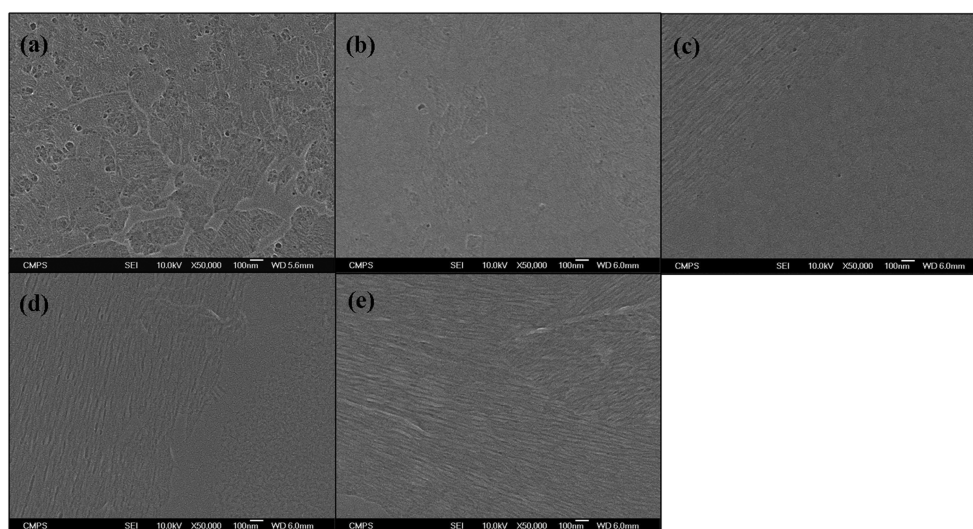


Fig. 2. SEM images of the PEDOT films at different THF solvent wt. % (a) 0 wt. %, (b) 25 wt. %, (c) 50 wt. %, (d) 75 wt. % and (e) 100 wt. % in THF-EtOH binary solvent.

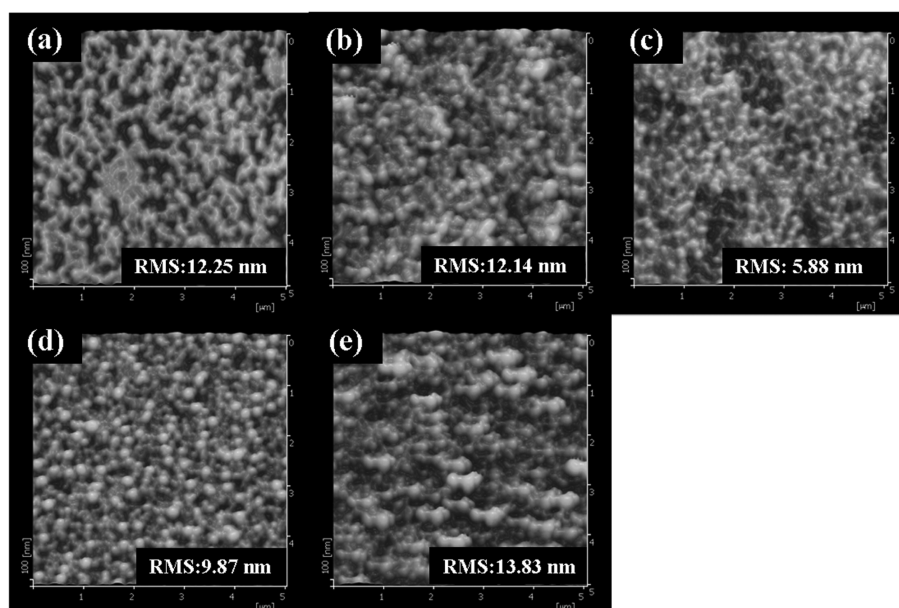


Fig. 3. AFM surface images of PEDOT films using THF-EtOH binary solvent mixtures at different THF solvent wt. % (a) 0 wt. %, (b) 25 wt. %, (c) 50 wt. %, (d) 75 wt. % and (e) 100 wt. %.

the microstructure and resulting surface morphology.

Figure 3 shows AFM surface images of PEDOT films deposited on the spin-coated FeCl_3 oxidant film with the binary EtOH-THF solvents. The RMS value of the PEDOT film deposited on the oxidant with pure EtOH was 13.83 nm. This value decreased slightly with an increase of the THF:EtOH wt. ratio to 0.25. When the ratio was increased further to 0.5, the RMS value decreased and reached a minimum (5.8 nm RMS), indicating the presence of an optimum THF/EtOH ratio to produce smooth surface PEDOT films. This is consistent with the observation of the smoothest surface morphology and highest conductivity of the PEDOT film obtained at THF:EtOH = 0.5, as shown in Figs. 1 and 2.

RBS was used to examine the solvent dependence of the thickness and stoichiometry of the FeCl_3 spin-coated film. Figure 4 shows the RBS spectra of the 3 wt. % FeCl_3 spin coated film with (a) EtOH and (b) THF-EtOH (50-50) mixed solvent. A simulation of the RBS spectra of the spin-coated FeCl_3 film revealed a multilayered structure consisting of $\text{Fe}_4\text{Cl}_{2.2}\text{C}_3\text{O}_{11}$ (45 nm) / $\text{Fe}_{0.1}\text{Cl}_{0.1}\text{C}_{0.1}\text{O}_6\text{Si}_3$ (40 nm) / SiO_2 (100 nm) / Si-substrate for pure EtOH and $\text{Fe}_4\text{Cl}_{2.7}\text{C}_{10}\text{O}_3$ (70 nm) / $\text{Fe}_{0.1}\text{Cl}_{0.1}\text{C}_2\text{O}_4\text{Si}_2$ (40 nm) / SiO_2 (100 nm) / Si-substrate for the mixed solvent. In order to properly fit the RBS data, additional layers, for example, $\text{Fe}_{0.1}\text{Cl}_{0.1}\text{C}_{0.1}\text{O}_6\text{Si}_3$ (40 nm) and $\text{Fe}_{0.1}\text{Cl}_{0.1}\text{C}_2\text{O}_4\text{Si}_2$ (40 nm), were needed in the simulated layers, possibly due to simulation of rough surfaces of the spin coated FeCl_3 films.

Compared to the pure EtOH solvent, the film spin-coated with the mixed solvent was thicker. This was due to the higher evaporation rate of the mixed solvent relative to that of pure EtOH. According to Meyerhofer's equation, increas-

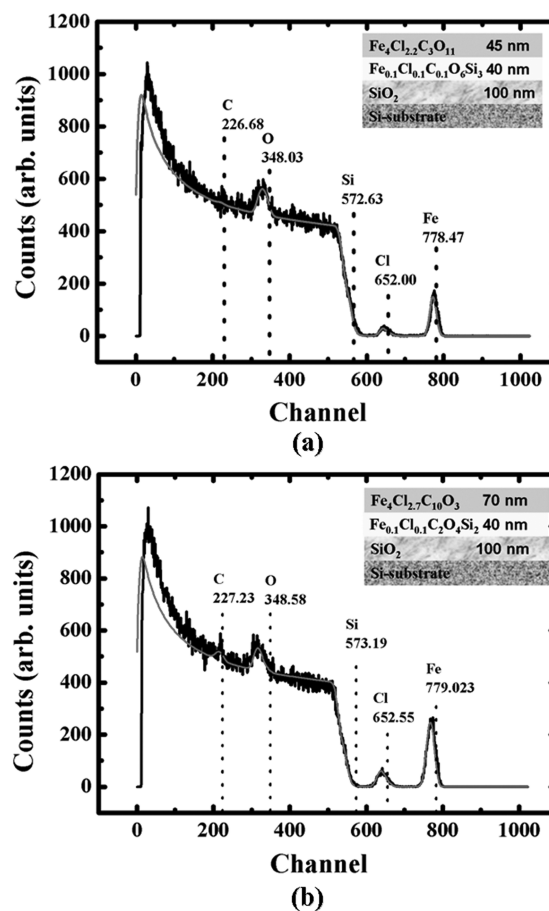


Fig. 4. RBS spectra of the spin-coated FeCl_3 film using (a) Pure EtOH solvent and (b) THF-EtOH (50-50) wt. % mixed solvent (simulated structure is shown inset).

ing the evaporation rate increases the final thickness of the resulting spin-coated films.^[19] The evaporation rate is closely related to the boiling point of the solvent. For example, a higher boiling point solvent has a slower evaporation rate than a lower boiling point solvent. As a result, the lower boiling point of THF (boiling points of THF and EtOH are 66°C and 78.4°C, respectively^[20]) increases the spin-coated film thickness.

Figure 5 shows the RBS intensities of the elements in the FeCl₃ films spin coated with pure EtOH and the mixed solvent. Regarding Fe and Cl, wider channels were observed in the 50:50 mixed-solvent FeCl₃ film than in the pure EtOH-solvent film, indicating a thicker FeCl₃ film is obtained with the mixed solvent. In addition, a significant amount of C was observed in both films, likely due to the presence of solvent molecules in the final spin-coated films. Moreover, there was a larger amount of carbon in the FeCl₃ film with the mixed solvent than with the pure EtOH solvent, indicating the presence of more solvent in the spin-coated film. Regarding the oxygen content, a larger amount of oxygen was observed in the FeCl₃ films with the EtOH solvent than those with the mixed solvent, possibly due to the higher oxidation of FeCl₃ during exposure to ambient conditions.

THF is a stronger ligand than EtOH.^[21] As the concentration of THF in the binary solvent is increased, it can replace the Cl in FeCl₃ to produce FeCl_x(THF)_y, which reduces the

formation of iron oxides. It was previously reported that, in the case of EtOH, the porous structure of the PEDOT films was due to facile crystallite formation of Fe₂O₃ or aggregation of iron in the film.^[22]

FT-IR spectroscopy was used to characterize the PEDOT films. Figure 6 shows the FTIR spectra of the PEDOT films deposited on the FeCl₃ oxidant films with pure EtOH and with the mixed solvent at a THF:EtOH ratio of 1. The peak at approximately 1320 cm⁻¹ was assigned to conjugated C-C / C=C bond stretching of the quinoidal structure of the thiophene ring.^[23-26] The two PEDOT films showed a difference in intensity of the peak at 1320 cm⁻¹, which was reported to be the main characteristic peak of a doped PEDOT film. The PEDOT film deposited with the THF-EtOH (50-50 wt. %) binary solvent showed a higher intensity peak than the pure EtOH solvent, revealing a longer PEDOT chain length. In addition, the peaks at 2860 cm⁻¹ to 2980 cm⁻¹ were assigned to CH₂ vibrations due to the 2,5-hydrogen atoms on the thiophene ring of the monomer. This suggests a broken conjugated bond to produce short-chained PEDOT. The intensity of the peaks (2860 cm⁻¹ to 2980 cm⁻¹) increased in the PEDOT film deposited with the pure EtOH solvent, indicating a larger amount of short chain PEDOT.^[27]

The PEDOT films deposited on the APS monolayer with the mixed solvent initially showed poor adhesion to the APS monolayer, but the adhesiveness improved with time. It was

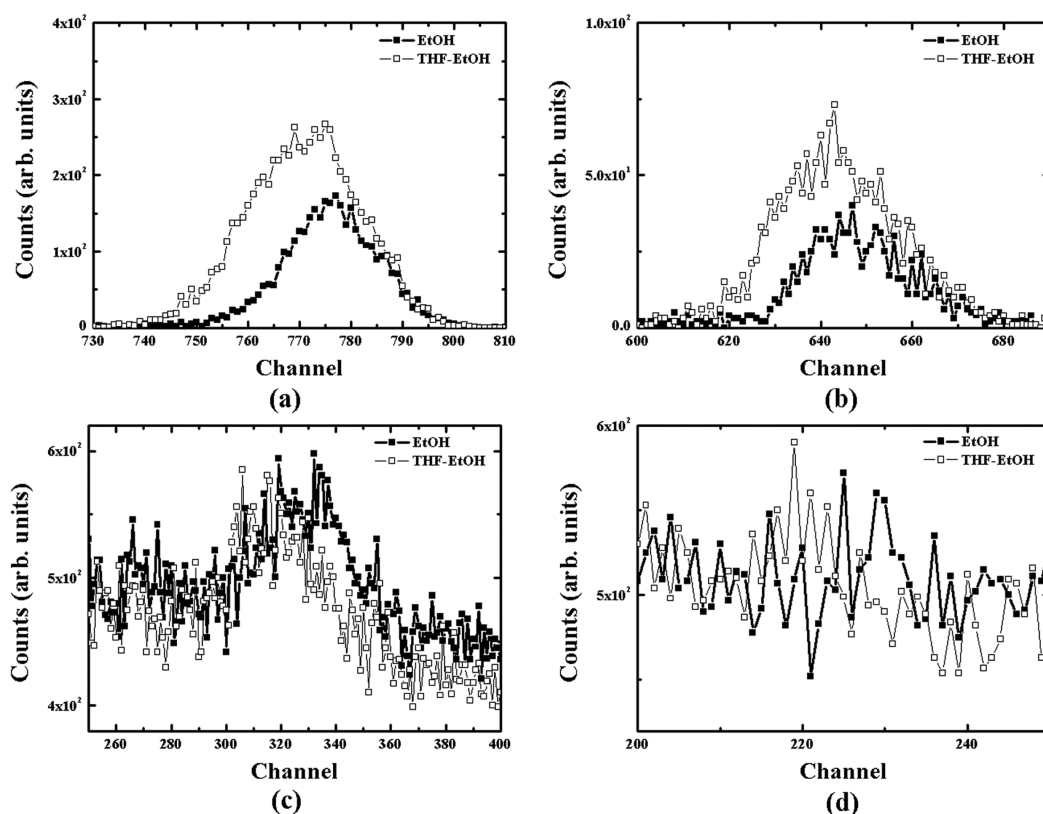


Fig. 5. RBS intensities of the elements in spin coated FeCl₃ films for pure EtOH and mixed solvent (a) Fe, (b) Cl, (c) O, and (d) C.

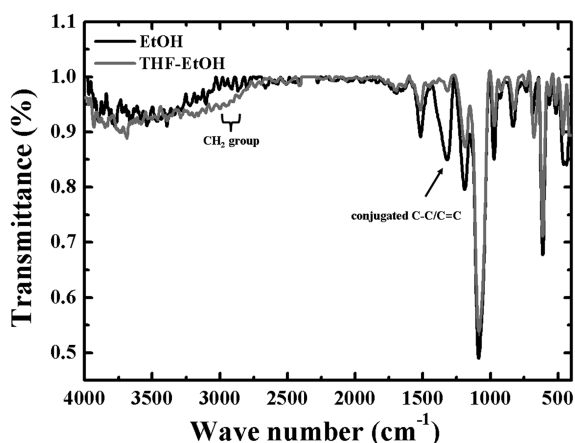
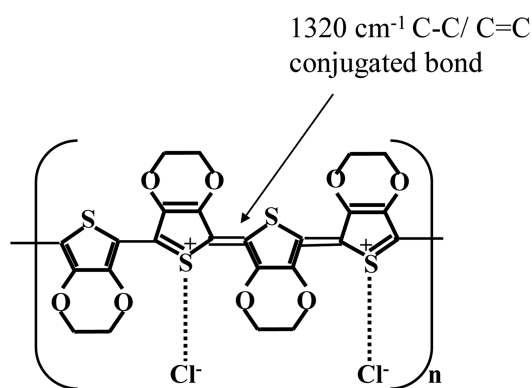


Fig. 6. FTIR scans of the PEDOT films are formed using (a) pure EtOH and (b) EtOH-THF mixed solvent.



Scheme 1. Quinoidal like Doped PEDOT structure, Cl^- (dopant).

previously reported that Fe^{3+} could break the dioxan bond of PEDOT at the interface to create a new bond with APS. Therefore, it is believed that the strong interaction between Fe^{3+} and the amine group of the APS monolayer is essential for robust adhesion.^[28] However, THF shielded Fe^{3+} by surrounding the ion, which reduced the interactions between the amine surface group and Fe^{3+} , leading to poor adhesion. The strong adhesion resumed approximately two days after deposition, possibly due to newly formed bonds between APS and the PEDOT film.^[28]

4. CONCLUSIONS

The solvent molecules included in the spin-coated FeCl_3 oxidant film affected the formation of PEDOT films on the oxidant films through oxidative chemical polymerization of EDOT. The addition of THF to EtOH solvent increased the amount of solvent in the spin-coated FeCl_3 films, and also improved the surface morphology of the resulting PEDOT films, leading to enhanced conductivity up to THF:EtOH = 1. Further increases in the ratio degraded the surface morphol-

ogy and conductivity, indicating the existence of an optimum THF:EtOH ratio to produce high quality PEDOT films.

ACKNOWLEDGMENTS

This work was supported by the Science Research Center / Engineering Research Center (SRC/ERC) program of the Ministry of Education, Science and Technology / Korea Science and Engineering Foundation (MEST/KOSEF) (R11-2005-048-00000-0). This work was also supported by the 2008 research program of Kookmin University in Korea.

REFERENCES

1. M. Halik, H. Klauk, U. Zschieschang, G. Schmid, W. Radlik, and W. Weber, *Adv. Mater.* **14**, 1717 (2002).
2. S. Admassie, F. Zhang, A. G. Manoj, M. Svensson, M. R. Andersson, and O. Inganäs, *Sol. Energy Mater. Sol. Cells* **90**, 133 (2006).
3. H. Mu, W. Li, R. Jones, A. Steckl, and D. Klotzkin, *J. Lumin.* **126**, 225 (2007).
4. F. L. Zhang, M. Johansson, M. R. Andersson, J. C. Hummelen, and O. Inganäs, *Adv. Mater.* **14**, 662 (2002).
5. S. H. Lee, J. H. Kim, T. H. Shim, and J. G. Park, *Electron. Mater. Lett.* **5**, 47 (2009)
6. S. Kirchmeyer, and K. Reuter, *J. Mater. Chem.* **15**, 2077 (2005).
7. B. B. Groenendaal, F. Jonas, D. Freitag, H. Pielartzik, and J. R. Reynolds, *Adv. Mater.* **12**, 481 (2000).
8. Y. Wang, *J. Phys.: Conf. Ser.* **152**, 012023 (2009).
9. H. Park, S. Go, K. Lee, and J. Lee, *Electron. Mater. Lett.* **4**, 181 (2008)
10. S. H. Cho and P. K. Song, *Met. Mater. Int.* **14**, 505 (2008)
11. T. Y. Kim, J. E. Kim, K. S. Suh, *Polym Int* **55**, 80 (2006).
12. Y. Xiao, X. Cui, and D. C. Martin, *J. Electroanal. Chem.* **573**, 43 (2004).
13. B. Winther-Jensen and K. West, *Macromolecules* **37**, 4538 (2004).
14. S. K. M. Jonsson, J. Birgeron, X. Crispin, G. Greczynski, W. Osikowicz, A. W. D. Gon, W. R. Salaneck, and M. Fahlman, *Syn. Met.* **139**, 1 (2003).
15. T. Y. Kim, C. M. Park, J. E. Kim, and K. S. Suh, *Syn. Met.* **149**, 169 (2005).
16. A. M. Nardes, R. A. J. Janssen, and M. Kemerink, *Adv. Funct. Mater.* **18**, 865 (2008).
17. Y. H. Ha, N. Nikolov, S. K. Pollack, J. Mastrangelo, B. D. Martain, and R. Shashidhar, *Adv. Funct. Mater.* **14**, 615 (2004).
18. J. Y. Kim, J. H. Jung, D. E. Lee, and J. Joo, *Syn. Met.* **126**, 311 (2002).
19. D. Meyerhofer, *J. Appl. Phys.* **49**, 3993 (1978).
20. D. R. Lide, *CRC Handbook of Chemistry and Physics* (76th ed.), p. 6-246, CRC Press, Boca Raton (1995)
21. H. Takagi, T. Isoda, K. Kusakabe, and S. Morooka, *Energy*

- Fuels* **13**, 1191 (1999).
22. M. A. Ali, H. H. Kim, C. Y. Lee, H. S. Soh, and J. G. Lee, *Met. Mater. Int* **15**, 977 (2009).
23. J. W. Choi, M. G. Han, S. Y. Kim, S. G. Oh, and S. S. Im, *Syn. Met.* **141**, 293 (2004).
24. J. P. Lock, S. G. Im, and K. K. Gleason, *Macromolecules* **39**, 5326 (2006).
25. C. Kvarnstrom, H. Neugebauer, A. Ivaska, and N. S. Saric-iftci, *J. Mol. Struct.* **521** 271 (2000).
26. Y. Xiao, X. Cui, and D. C. Martin, *J. Electroanal. Chem.* **573**, 43 (2004).
27. M. Fabretto, K. Zuber, C. Hall, and P. Murphy, *Macromol. Rapid Commun.* **29** 1403 (2008).
28. S. Kim, I. Pang, and J. Lee, *Macromol. Rapid Commun.* **28**, 1574 (2007).
25. C. Kvarnstrom, H. Neugebauer, A. Ivaska, and N. S. Saric-